

## THE QUANTUM DOTS SOLAR CELLS BASED-ON DIFFERENT COUNTER ELECTRODES

**Tung Ha Thanh<sup>\*</sup>, Nguyen Thanh Nguyen**

*Faculty of Physics, Dong Thap University, Dong Thap province*

<sup>\*</sup>Email: [httung@dthu.edu.vn](mailto:httung@dthu.edu.vn)

Received: 25 May 2014; Accepted for publication: 9 February 2015

### ABSTRACT

Solar cells based on a mesoporous structure of TiO<sub>2</sub> and the polysulfide redox electrolyte were prepared by direct adsorption of CdS/CdSe/ZnS quantum dots (QDs) light absorbers onto the oxide. Moreover, we also synthesized quantum dots solar cells (QDSSCs) based on different counter electrodes like CuS, Cu<sub>2</sub>S, PbS by successive ionic layer adsorption and reaction (SILAR) method and chemical bath deposition (CBD). The performance photovoltaic was about 0.87 % for Cu<sub>2</sub>S counter electrode, i.e. higher than other counter electrodes. With this result, CuS, Cu<sub>2</sub>S and PbS exhibit several advantages in which they can replace Pt commercial in the future.

*Keywords:* counter electrodes; quantum dots; solar cells.

### 1. INTRODUCTION

Nowadays, there exists an intense effort aimed at developing third-generation solar cells. One of the most promising approaches involves the use of semiconductor quantum dots (QDs) as light absorbers. QDs exhibit attractive characteristics as sensitizers due to their tunable bandgap [1] by size control, which can be used to match the absorption spectrum to the spectral distribution of solar light. Additionally, QDs possess higher extinction coefficients [1, 2], compared to metal–organic dyes, and large intrinsic dipole moment leading to rapid charge separation [3, 4]. The demonstration of multiple exciton generation by impact ionization [5, 6] has fostered interest in colloidal quantum dots. One of the most attractive configurations to exploit these fascinating properties of QDs is the quantum-dot-sensitized solar cell (QDSC) [7, 8]. The optimization of QDSCs can benefit from the intensive effort carried out with dye-sensitized solar cells (DSCs) [9].

Recently, Lee et al. have reported a self-assembled TiO<sub>2</sub>/CdS/CdSe structure that exhibited a significant enhancement in the photocurrent response [10,11]. In addition, nanostructured CuS, PbS, and Cu<sub>2</sub>S have been used as electrocatalysts on the counter electrodes. Alternative catalysts have been proposed by several researchers [10–13]. Metal sulfides are considered as good choice. However, their deposition on plain FTO electrodes does not always produce materials with sufficiently high specific surface or with structural stability.

In this letter, we studied the effects of co-modification by CdS, CdSe and ZnS QDs on the photovoltaic response of mesoporous TiO<sub>2</sub> based QDSSC. The mesoporous TiO<sub>2</sub> were treated by SILAR of CdS, CdSe and ZnS QDs and were used as photoanodes in QDSSC. We demonstrated that the comodified mesoporous TiO<sub>2</sub> possess superior photovoltaic response compared to the single QD sensitized devices. Pt, CuS, PbS and Cu<sub>2</sub>S have been used as electrocatalysts on counter electrodes. The final TiO<sub>2</sub>/CdS/CdSe/ZnS photoanode leads to high efficiency QDSSCs.

## **2. EXPERIMENT**

### **2.1. Materials**

Cd(CH<sub>3</sub>COO)<sub>2</sub>·2H<sub>2</sub>O (99 %), Cu(NO<sub>3</sub>)<sub>2</sub>, Na<sub>2</sub>S, Zn(NO<sub>3</sub>)<sub>2</sub>, Se powder, S powder, Na<sub>2</sub>SO<sub>3</sub>, Brass foil obtained from Merck. TiO<sub>2</sub> paste obtained from Dyesol, Australia and SnO<sub>2</sub>:F transparent conductive electrodes (FTO, resistance 8 Ω/square) were purchased from Pilkington.

### **2.2. To prepare TiO<sub>2</sub> films**

The TiO<sub>2</sub> thin films were fabricated by silk-screen printing with commercial TiO<sub>2</sub> paste. Their sizes ranged from 10 to 20 nm. Two layers of film with thickness of 8 μm (measured by microscope). Then, the TiO<sub>2</sub> film was heated at 400 °C for 5 min, 500 °C for 30 min. Afterward, the film was dipped in 40-mmol TiCl<sub>4</sub> solution for 30 min at 70 °C and heated at 500 °C for 30 min. The specific surface area of the mesoporous TiO<sub>2</sub> were investigated by using the N<sub>2</sub> adsorption and desorption isotherms before and after the calcination. The surface area is 120.6 m<sup>2</sup>g<sup>-1</sup> (measured by BET devices). This result indicates that the synthesized material has wider mesoporous structure.

### **2.3. To prepare TiO<sub>2</sub>/CdS/CdSe/ZnS films**

The highly ordered TiO<sub>2</sub> were sequentially sensitized with CdS, CdSe and ZnS QDs by SILAR method. First, the TiO<sub>2</sub> film was dipped in 0.5 mol/L Cd(CH<sub>3</sub>COO)<sub>2</sub>-ethanol solution for 5 min, rinsed with ethanol, dipped for 5 min in 0.5 mol/L Na<sub>2</sub>S-methanol solution and then rinsed with methanol. The two-step dipping procedure corresponded to one SILAR cycle and the incorporated amount of CdS QDs was increased by repeating the assembly cycles for a total of three cycles. For the subsequent SILAR process of CdSe QDs, aqueous Se solution was prepared by mixing Se powder and Na<sub>2</sub>SO<sub>3</sub> in 50 ml pure water, after adding 1 mol/L NaOH at 70 °C for 7 h. The TiO<sub>2</sub>/CdS samples were dipped into 0.5 mol/L Cd(CH<sub>3</sub>COO)<sub>2</sub>-ethanol solution for 5 min at room temperature, rinsed with ethanol, dipped in aqueous Se solution for 5 min at 50 °C, rinsed with pure water. The two-step dipping procedure corresponds to one SILAR cycle. Repeating the SILAR cycle increases the amount of CdSe QDs (a total of four cycles). The SILAR method was also used to deposit the ZnS passivation layer. The TiO<sub>2</sub>/CdS/CdSe samples were coated with ZnS by alternately dipping the samples in 0.1 mol/L Zn(NO<sub>3</sub>)<sub>2</sub> and 0.1 mol/L Na<sub>2</sub>S-solutions for 5 min/dip, rinsing with pure water between dips (a total of two cycles). Finally, it was heated in a vacuum environment with different temperatures to avoid oxidation (see Figure. 1). The TiO<sub>2</sub>/CdS/CdSe/ZnS was be measured thickness by microscopic. The results of the average thickness of CdS(1), CdSe(1), ZnS(1) are 40 nm, 43.3 nm, 40 nm respectively.

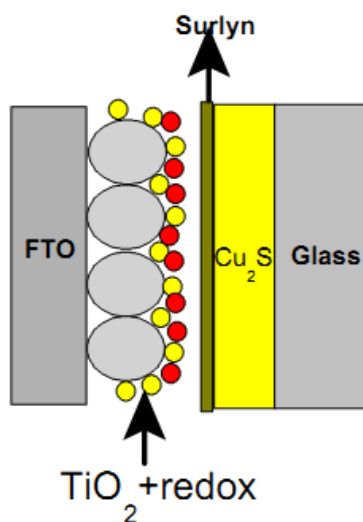


Figure 1. The diagram shows the process to prepare the solar cells.

#### 2.4. Construction of the counter electrodes

PbS films were deposited on fluorine doped tin oxide (FTO) conductive glass electrode by cyclic voltammetry (CV) from the solution of  $\text{Pb}(\text{NO}_3)_2$  1.5 mM and  $\text{Na}_2\text{S}_2\text{O}_3$  1.5 mM. CV experiments were carried out at various potential scan rates in a potential range 0.0 to  $-1.0$  V versus Ag/AgCl/KCl electrode, pH from 2.4 to 2.7 and ambient temperature. Pt films were fabricated by silk-screen printing with commercial Pt paste. Then, the Pt films were heated at  $450^\circ\text{C}$  for 30 min. CuS was also deposited on FTO electrodes by a SILAR procedure, by modifying the method presented in Ref. [14]. Precursor solutions contained 0.5 mol/L  $\text{Cu}(\text{NO}_3)_2$  in methanol and 1 mol/dm<sup>3</sup>  $\text{Na}_2\text{S}\cdot 9\text{H}_2\text{O}$  in a 1:1 water:methanol mixture.

A FTO electrode was immersed for 5 min in the metal salt solution, then copiously washed with triple-distilled water and dried in an air stream, then immersed for 5 min in the  $\text{Na}_2\text{S}\cdot 9\text{H}_2\text{O}$  solution and finally washed and dried again. This sequence again corresponds to one SILAR cycle. 10 SILAR cycles were performed. Finally, the electrode with deposited CuS film was first dried and then it was put for 5 min in an oven at  $100^\circ\text{C}$ . The counter electrode was a  $\text{Cu}_2\text{S}$  film fabricated on brass foil. Brass foil was immersed into 37 % HCl at  $70^\circ\text{C}$  for 5 min, then rinsed with water and dried in air. After that, the etched brass foil was dipped into 1 mol/L S and 1 mol/L  $\text{Na}_2\text{S}$  aqueous solution, resulting in a black  $\text{Cu}_2\text{S}$  layer forming on the foil [15].

#### 2.5. Fabrication of QDSSCs

The polysulfide electrolyte used in this work was prepared freshly by dissolving 0.5 M  $\text{Na}_2\text{S}$ , 0.2 M S, and 0.2 M KCl in Milli-Q ultrapure water/methanol (7:3 by volume). The CdS/CdSe/ZnS co-sensitized  $\text{TiO}_2$  photoanode and counter electrode (CE) were assembled into a sandwich cell by heating with a Surlyn. The electrolyte was filled from a hole made on the CE, which was later sealed by thermal adhesive film and a cover glass. The active area of QDSSC was  $0.38\text{ cm}^2$ .

#### 2.6. Characterizations and measurements

The morphology of the prepared samples was observed using field-emission scanning electron microscopy (FE-SEM, S4800). The crystal structure was analyzed by an X-ray diffractometer (Philips, Panalytical X'pert, CuK $\alpha$  radiation). The absorption properties of the samples were investigated by a diffuse reflectance UV–vis spectrometer (JASCO V-670). Photocurrent – voltage measurements were performed on a Keithley 2400 sourcemeter using a simulated AM 1.5 sunlight with an output power of 100 mW/cm<sup>2</sup> produced by a solar simulator (Solarena, Sweden).

### 3. RESULTS AND DISCUSSION

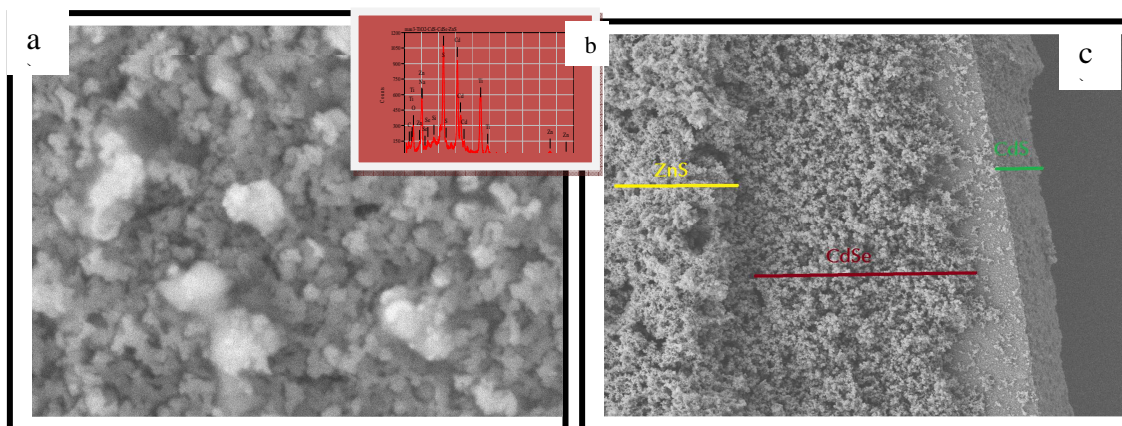


Figure 2. (a) FE-SEM images of the TiO<sub>2</sub>/CdS/CdSe/ZnS photoanode, (b) energy dispersive spectra (EDS) of the TiO<sub>2</sub>/CdS/CdSe/ZnS photoanode, and (c) FE-SEM images cross-sectional view of the TiO<sub>2</sub>/CdS/CdSe/ZnS photoanode.

Shown in Fig. 2(a) and 2(c) are the FESEM of TiO<sub>2</sub>/CdS/CdSe/ZnS photoanode. Fig. 2a shows highly uniform porous morphology with the average inner diameter of nano structure around 60 nm. For photovoltaic applications, the structure of QDs adsorbed TiO<sub>2</sub> should meet at least two criteria. First, the QDs should be uniformly deposited onto the TiO<sub>2</sub> surface without aggregation, so that the area of TiO<sub>2</sub>/QDs can be maximized. Second, a moderate amount the QDs should be deposited so that the TiO<sub>2</sub> are not blocked. Fig. 2(c) is a cross sectional image showing that the QDs are well deposited onto the TiO<sub>2</sub> with an average thickness of about 12  $\mu$ m by the microscope. Fig. 2 (b) is the energy dispersive spectra of the TiO<sub>2</sub>/CdS/CdSe/ZnS film. It shows that the Ti and O peaks are from the TiO<sub>2</sub> film; and Cd, Se, Zn and S peaks, clearly visible in the EDS spectrum, are from the QDs. The Si is from the FTO and C is from the solvent organic. That shows, the QDs are well deposited onto the TiO<sub>2</sub>.

The structure of the TiO<sub>2</sub>/QDs photoelectrodes for photovoltaic applications, shown in Fig. 3(a), are studied by the XRD patterns. It reveals that the TiO<sub>2</sub> have an anatase structure with a strong (101) peak located at 25.4 $^{\circ}$ , which indicates that the TiO<sub>2</sub> films are well crystallized and grow along the [101] direction (JCPDS Card no. 21-1272). Three peaks can be observed at 26.4 $^{\circ}$ , 44 $^{\circ}$  and 51.6 $^{\circ}$ , which can be indexed to (111), (220) and (331) of cubic CdS (JCPDS Card no. 41-1049), CdSe (JCPDS Card no. 75-5681) respectively. Moreover, two peaks can be observed at 48 $^{\circ}$  and 54.6 $^{\circ}$  that can be indexed to (220) and (331) of cubic ZnS respectively. So, It demonstrates that the QDs have crystallized onto the TiO<sub>2</sub> film. Fig. 3(b) is the raman spectrum of the TiO<sub>2</sub>/QDs photoelectrodes where It shows that an anatase structure of the TiO<sub>2</sub>

films have five oscillation modes corresponding with wave numbers at 143, 201, 395, 515 and 636  $\text{cm}^{-1}$ . In addition, we can see two peaks at 201 and 395  $\text{cm}^{-1}$  of CdSe cubic, a peak at 298  $\text{cm}^{-1}$  of CdS cubic and a peak at 361  $\text{cm}^{-1}$  of ZnS cubic. The results of the raman is likely the results of XRD. The optical performance of the QDs coated  $\text{TiO}_2$  film is characterized by absorbance. Fig. 3(c) shows the UV-Vis absorption spectra of thus sensitized electrodes measured after SILAR. As expected, the absorbance is about 496 nm which shifted to long-wavelength region due to more co-absorption of CdS, CdSe and ZnS which loaded on  $\text{TiO}_2$  film.

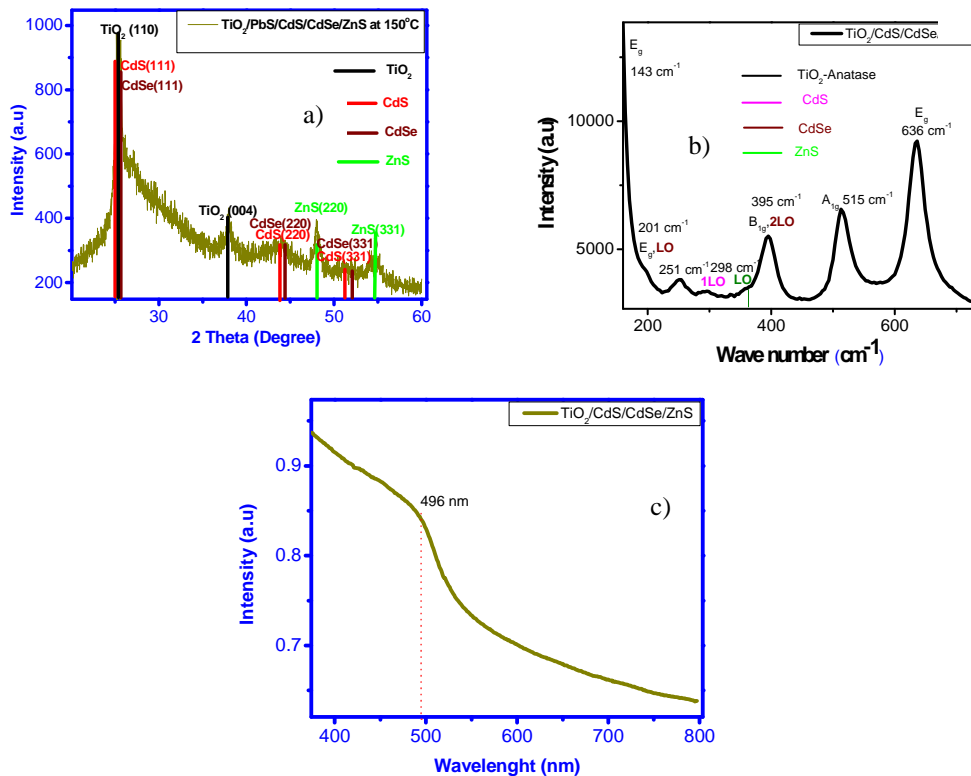


Figure 3. (a) XRD, (b) Raman and (c) UV-Vis spectra of  $\text{TiO}_2/\text{CdS}/\text{CdSe}/\text{ZnS}$  photoanode.

The XRD patterns was used to characterize the crystall structure. As shown in Fig. 4a, it can be seen that the XRD pattern of the PbS counter electrode is in conformity with cubic ( $a=b=c= 5.93 \text{ \AA}$ ). The observed peaks could be assigned to diffraction from the (111), (200), (220), (311), (222)... faces and there is no characteristic peak for other impurities. This indicates that pure crystalline PbS was formed via the cyclic voltametry process. Fig. 4c illustrates the XRD pattern of the synthesized  $\text{Cu}_2\text{S}$  after 1h by Chemical bath deposition (CBD) method. The peaks of corresponding crystal planes were indexed in the figure, matching to the hexagonal phase chalcocite  $\beta\text{-Cu}_2\text{S}$  (JCPDS card no. 46-1195,  $a = 3.96 \text{ \AA}$ ,  $c = 6.78 \text{ \AA}$ ). As shown in Fig. 4e, it can be seen that the XRD pattern of the CuS counter electrode is in conformity with the hexagonal phase. It are in agreement with the reported data for CuS (JCPDS Card. No. 79-2321). Fig. 4b, 4d, 4f show the FE-SEM image of PbS,  $\text{Cu}_2\text{S}$ , CuS films to present a rough nanostructure which are suitable for counter electrodes.

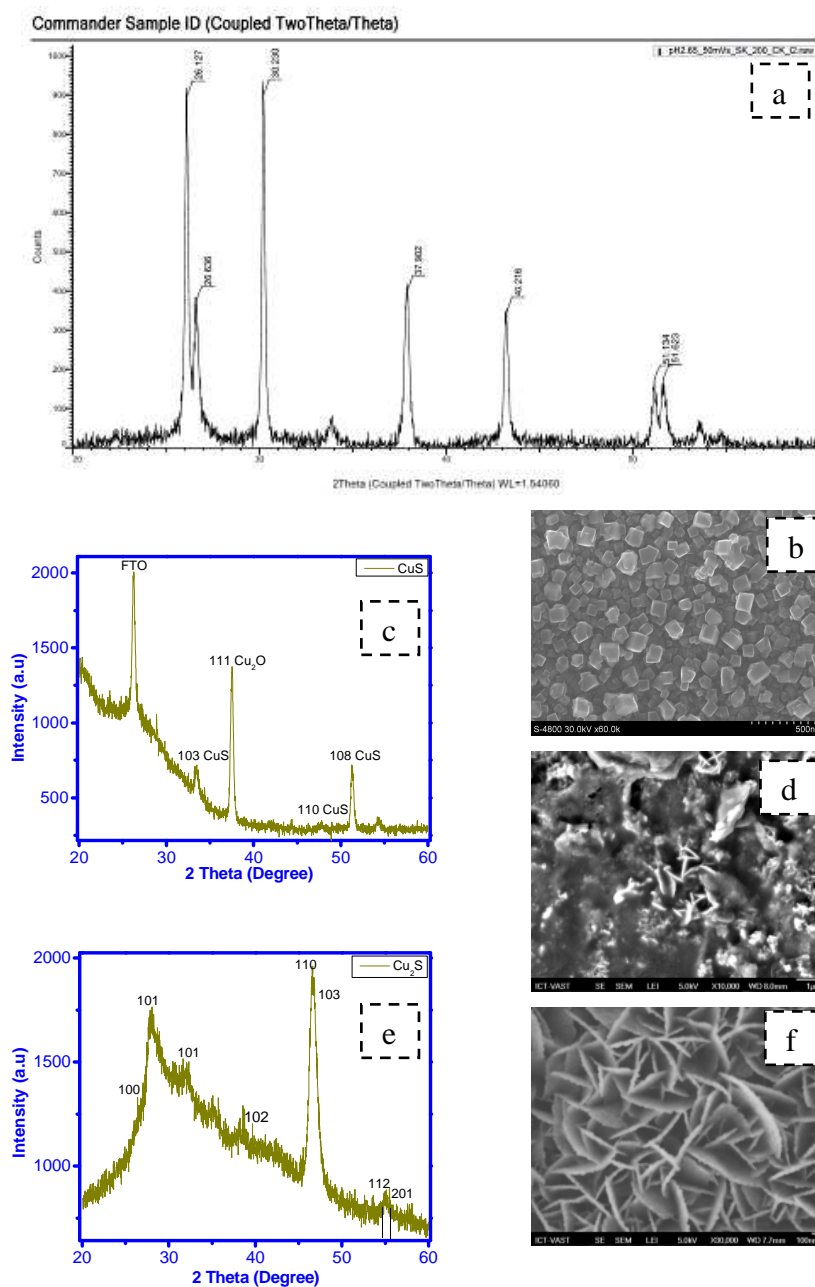


Figure 4. XRD and FESEM of (a-b) PbS, (c-d) Cu<sub>2</sub>S and (e-f) CuS counter electrodes.

A relative energy level of different components is shown in Fig. 5. According to the data reported in the literatures [17,18], the band gap of TiO<sub>2</sub> (3.2 eV) limits its absorption range below the wavelength of about 400 nm. CdSe has a higher conduction band (CB) edge than TiO<sub>2</sub>, which is favorable for electron injection. However, with a band gap of 1.7 eV, the absorption of bulk CdSe is also limited below approximately 760 nm. The conduction band of CdSe is slightly lower than that of TiO<sub>2</sub>, so the electrons would flow from CdSe to TiO<sub>2</sub> [19]. In addition, we have coated two layers ZnS QDs, which could be attributed to several reasons.

First, as the absorption edge of ZnS is at about 345 nm, a higher absorption can be obtained due to the complement of the absorption spectrum of the ZnS with that of the CdSe and CdS QDs. Second, ZnS acts as a passivation layer to protect the CdS and CdSe QDs from photocorrosion. Thus, the photoexcited electrons can efficiently transfer into the conduction band of TiO<sub>2</sub>.

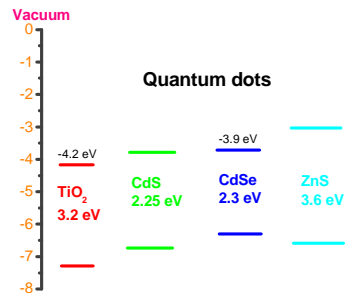


Figure 5. The proposed energy band structure of the TiO<sub>2</sub>/CdS/CdSe/ZnS nano structure interface. All the energy levels are referenced to NHE scale. CB and VB are conduction band and valence band.

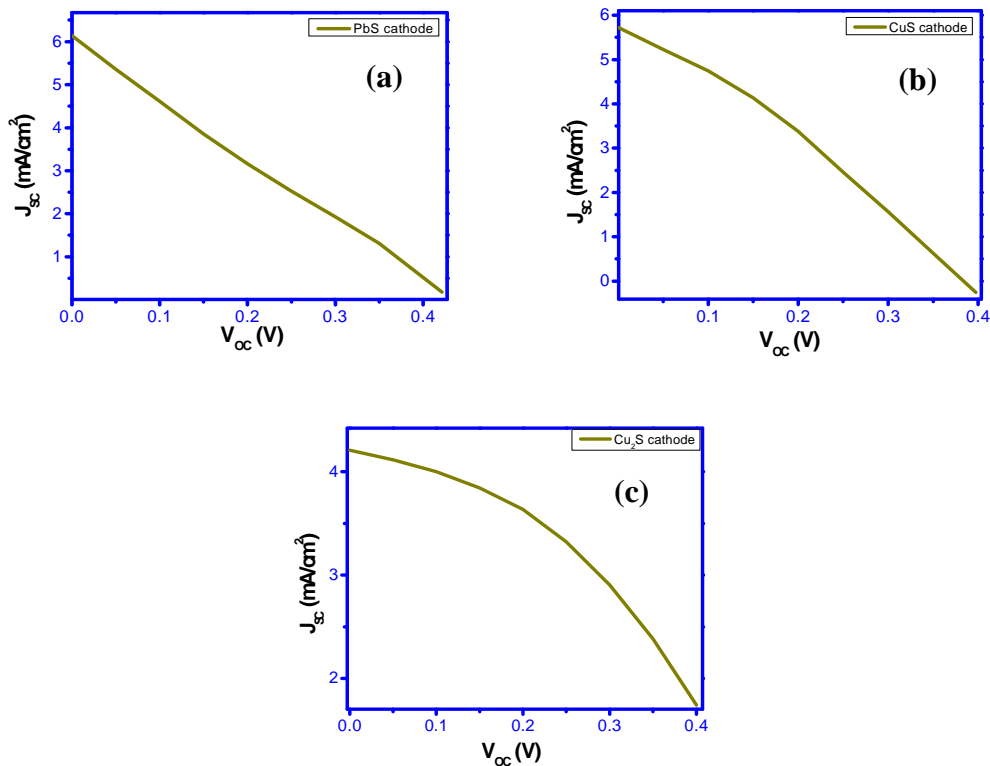


Figure 6. J–V curves of solar cells modified by various cathodes.

Third, the outer ZnS layer can also be considered to be a potential barrier between the interface of QDs materials and the electrolyte. ZnS has a very wide band gap of 3.6eV, it is much wider than that on the CdS and CdSe QDs. As a result, the leakage of electrons from the ZnS, CdSe and CdS QDs into the electrolyte can be inhibited. As a result, an ideal model for the cosensitized TiO<sub>2</sub> electrode is shown in Fig. 5b. After the CdSe and ZnS QDs are sequentially

deposited onto a TiO<sub>2</sub>/CdS film, A cascade type energy band structure is constructed for the cosensitized photoanode. The best electron transport path is from the conduction band of ZnS and finally reaching the conduction band of TiO<sub>2</sub>. Meanwhile, this stepwise structure is also favorable for the hole transport.

Three main types of counter electrodes have been studied. Their synthesis is detailed in experiment and method. In the first case, PbS films were deposited on fluorine doped tin oxide (FTO) conductive glass electrode by cyclic voltammetry (CV) from the solution of Pb(NO<sub>3</sub>)<sub>2</sub> 1.5 mM and Na<sub>2</sub>S<sub>2</sub>O<sub>3</sub> 1.5 mM. CV experiments were carried out at various potential scan rates in a potential range 0.0 to -1.0 V versus Ag/AgCl/KCl electrode, pH from 2.40 to 2.70 and ambient temperature. CuS was also deposited on FTO electrodes by a SILAR procedure, by modifying the method presented in Ref. [14]. The electrode with deposited CuS film was first dried and then it was put for 5 min in an oven at 100°C. The counter electrode was a Cu<sub>2</sub>S film fabricated on brass foil. Brass foil was immersed into 37 % HCl at 70°C for 5 min, then rinsed with water and dried in air. After that, the etched brass foil was dipped into 1 mol/L S and 1 mol/L Na<sub>2</sub>S aqueous solution, resulting in a black Cu<sub>2</sub>S layer forming on the foil [15]. Fig. 4a, 4b, 4c shows J-V curves of solar cells based on PbS, CuS, Cu<sub>2</sub>S counter electrodes which shows that the maximum efficiency reached in the present work 0.87 % of efficiency obtained to Cu<sub>2</sub>S counter electrode. However, the PbS and CuS electrodes gave higher current densities than does Cu<sub>2</sub>S. On the contrary open-circuit voltage values were practically not affected by the electrocatalyst. The major problem encountered in the present work was with the value of the fill factor (FF). It remained below 0.42 and this limited the overall efficiency, even though, the current densities presently recorded were high. The search for a higher FF is an open question and has occupied many other researchers. It is believed that higher FFs will be obtained with even better electrocatalysts and more functional counter electrodes.

Table 2. Photovoltaic parameters of solar cell modified by various cathodes.

<i>Solar Cells</i>	<i>J<sub>SC</sub> (mA/cm<sup>2</sup>)</i>	<i>V<sub>OC</sub>(V)</i>	<i>Fill factor FF</i>	<i>efficiency η(%)</i>
<b>PbS cathode</b>	6.14	0.43	0.24	0.63
<b>CuS cathode</b>	5.72	0.38	0.31	0.68
<b>Cu<sub>2</sub>S cathode</b>	4.2	0.55	0.376	0.87

#### 4. CONCLUSIONS

QDSSCs have been constructed based on PbS, Cu<sub>2</sub>S and CuS which was used for electrocatalysts on counter electrodes in combination with a polysulfide electrolyte. The maximum solar conversion efficiency of 0.86 % was obtained with Cu<sub>2</sub>S counter electrode. However, the PbS and CuS electrodes gave higher current densities than does Cu<sub>2</sub>S. Finally, QDSSCs based on PbS, Cu<sub>2</sub>S and CuS obtained low performance photovoltaic because of low fill factor. This is the initial works which show us that these electrodes have many potential application in QDSSCs in the future.

**Acknowledgments.** This work was supported by the name of the project: CS2014.01.04 of Dong Thap University.



## REFERENCES

1. Yu W., Qu L. H., Guo W. Z and Peng X. G. - Experimental determination of the extinction coefficient of CdTe, CdSe and CdS nanocrystals, *Chem. Mater* **15** (2003) 2854
2. Wang P., Zakeeruddin S. M., Moser J. E., Humphry-Baker R., Comte P., Aranyos V., Hagfeldt A., Nazeeruddin M. K and Gratzel M. - A Solvent-Free, SeCN<sup>-</sup>/(SeCN)<sub>3</sub><sup>-</sup> Based Ionic Liquid Electrolyte for High-Efficiency Dye-Sensitized Nanocrystalline Solar Cells, *Journal of the American Chemical Society* **126** (2004) 7164-7165.
3. Vogel R., Pohl K and Weller H. - Sensitization of highly porous, polycrystalline TiO<sub>2</sub> electrodes by quantum sized CdS, *Chem. Phys. Lett* **174** (1990) 241
4. Vogel R., Hoyer P and Weller H. - Quantum-sized PbS, CdS, Ag<sub>2</sub>S, Sb<sub>2</sub>S<sub>3</sub> and Bi<sub>2</sub>S<sub>3</sub> particles as sensitizers for various nanoporous wide bandgap semiconductors, *J. Phys. Chem. B* **98** (1994) 3183
5. Schaller R. D., Sykora M., Pietryga J. M and Klimov V. I. - Mechanisms for photogeneration and recombination of multiexcitons in semiconductor nanocrystals, *J. Phys. Chem. B* **110** (2006) 25332.
6. Trinh M. T., Houtepen A. J., Schins J. M., Hanrath T., Piris J., Knulst W., Goossens A. P. L. M and Siebbeles L. D. A. - In spite of recent doubts carrier multiplication does occur in PbSe nanocrystals, *Nano Lett* **8** (2008) 1713
7. Klimov V. I. - Spectral and dynamical properties of multiexciton in semiconductor nanocrystals, *Annu. Rev. Phys. Chem* **58** (2007) 635-673.
8. Nozik A. - Quantum dot solar cells, *J. Physica E* **14** (2002) 115.
9. Regan B. O' and Gratzel M. - A low-cost, high-efficiency solar cell based on dye-sensitized colloidal TiO<sub>2</sub> films, *Nature* **353** (1991) 737.
10. Lee Y. L., Lo Y. S. - Highly efficient quantum-dot-sensitized solar cell based on co-sensitization of CdS/CdSe, *Adv. Funct. Mater* **19** (2009) 604-609.
11. Lee H. J., Bang J., Park J., Kim S, Park S. M. - Multilayered semiconductor (CdS/CdSe/ZnS)-sensitized TiO<sub>2</sub> mesoporous solar cells: all prepared by successive ionic layer adsorption and reaction processes, *Chemistry of Materials* **22**(2010), 5636-43.
12. Efros A. L., Rosen M., Kuno M., Nirmal M., Norris D. J., and Bawendi M. - Observation of the "dark exciton" in CdSe quantum dots, *Phys. Rev. B* **54** (1996), 4843.
13. Brus L. E. - A simple model for the ionization potential, electron affinity, and aqueous redox potentials of small semiconductor crystallites, *The Journal of Chemical Physics* **79** (1984) 5566-5572.
14. Li T. L., Lee Y. L., Teng H. - High-performance quantum dot-sensitized solar cells based on sensitization with CuInS<sub>2</sub> quantum dots/CdS heterostructure, *Energy and Environmental Science* **5** (2012) 5315.
15. Tian J., Gao R., Zhang Q., Zhang S., Li Y., Lan J., Qu X and Cao G. - A highly efficient (>6 %) Cd<sub>1-x</sub>MnxSe quantum dot sensitized solar cell, *J. Phys. Chem. C* **116** (2012) 18655-18662.
16. Tachan Z., Shalom M., Hod I., Ruhle S., Tirosh S and Zaban A. - PbS as a Highly Catalytic Counter Electrode for Polysulfide-Based Quantum Dot Solar Cells, *J. Phys. Chem C* **115** (2011) 6162.

17. Grätzel M. - Photoelectrochemical cells, *Nature* **414** (2001) 338–344.
18. Chris G. V., Neugebauer J. - Universal alignment of hydrogen levels in semiconductors, insulators and solutions, *Nature* **423** (2003) 626–628.
19. Lee Y. L., Lo Y. S. - Highly efficient quantum-dot-sensitized solar cell based on co-sensitization of CdS/CdSe, *Adv. Funct. Mater* **19** (2009) 604–609.

### **TÓM TẮT**

#### **PIN MẶT TRỜI CHẤM LƯỢNG TỬ TRÊN CƠ SỞ CÁC ĐIỆN CỰC CA TỐT KHÁC NHAU**

Hà Thanh Tùng\*, Nguyễn Thanh Nguyên

*Khoa Vật lý, Trường Đại học Đồng Tháp, tỉnh Đồng Tháp*

Email: [httung@dthu.edu.vn](mailto:httung@dthu.edu.vn)

Pin mặt trời chấm lượng tử được chế tạo trên cơ sở màng anốt  $\text{TiO}_2/\text{CdS}/\text{CdSe}/\text{ZnS}$  được chế tạo bằng phương pháp SILAR và các điện cực catốt CuS,  $\text{Cu}_2\text{S}$ , PbS được chế tạo bằng phương pháp ngâm hóa học. Kết quả hiệu suất thu được 0,85 % đối với ca tốt  $\text{Cu}_2\text{S}$  cao hơn so với pin trên cơ sở các điện cực catốt khác. Với kết quả thu được, pin mặt trời trên cơ sở các catốt  $\text{Cu}_2\text{S}$ , CuS, PbS hứa hẹn sẽ thay thế catốt Pt thương mại.

*Từ khóa:* điện cực catốt, chấm lượng tử, pin mặt trời.